

Contents lists available at ScienceDirect

Carbohydrate Polymer Technologies and Applications

journal homepage: www.sciencedirect.com/journal/carbohydrate-polymer-technologies-and-applications





Effect of poly(ethylene glycol)-based cross-linker length on the physicochemical and rheological properties of hyaluronic acid hydrogels potentially applicable in the biomedical field

Fabiana Cordella ^{a,b}, Giuseppe Alonci ^b, Gaetano Angelici ^a, Roberto Mocchi ^b, Martina Savona ^b, Giulia Grimaldi ^b, Giulia Galasso ^b, Sabrina Sommatis ^b, Celia Duce ^a, Elena Pulidori ^a, Elisa Martinelli ^{a,*}, Nicola Zerbinati ^{c,*}

ARTICLE INFO

Keywords:
Hyaluronic acid
Hydrogels
Dermal fillers
Crosslinkers
Chemical modification
Medical device
Rheology
Hydrogel characterization

The development of safe and effective hyaluronic acid-based materials is one of the main research focuses for biomedical applications. However, so far, an investigation of the influence of the cross-linker chain length on the physicochemical, mechanical, and rheological properties of the material has never been reported. Therefore, in the present work, a polydisperse poly(ethylene glycol) diglycidyl ether (PEGDE) and six monodisperse PEGDE with a well-defined length were successfully synthesized by a simple method and used as cross-linkers of hyaluronic acid to obtain hydrogels which differed only for the length of the cross-linker. Our results indicate that the cross-linking density, determined by using Flory-Rehner equation, and the total content of the cross-linker in the formulation, determined by 1 H NMR, decrease with PEGDE length. However, the formulations with the longer polydisperse PEGDEs ($n \geq 6$) exhibits a higher storage modulus (G' = 110.4–114.7 Pa) and a stiffer mechanical behaviour, indicating that cross-linker chain length influences significantly the rheological properties of hydrogels.

1. Introduction

In recent years, research on innovative materials for the clinic has been the subject of numerous studies in various biomedical fields, such as tissue engineering, wound healing, and aesthetic medicine, based on the rationale that interactions between proteins, nucleic acids, and polysaccharides determine the existence of major life processes (Todros et al., 2021). In particular, hyaluronic acid (HA), a glycosaminoglycan composed of repeating disaccharide units of alternating D-glucuronic acid and N-acetyl-D-glucosamine linked by β -1->4 and β -1->3 glycosidic bonds, is one of the most important constituents of the extracellular matrix, naturally present in skin and soft tissues, where it provides structural support and hydration due to its high affinity for water (Papakonstantinou, Roth, & Karakiulakis, 2012). The wide range of possible chemical modifications and its scalability through bacterial fermentation processes, avoiding the risks and complications of animal-derived products (Yasin, 2022; Schanté et al., 2011; Tiwari & Bahadur, 2019; Hintze, Schnabelrauch, & Rother, 2022), favoured its extensive use in cosmetic (Al-Halaseh et al., 2022) and numerous medical applications, such as ophthalmology (Huerta Ángeles & Nešporová, 2021), aesthetic medicine (Hong et al., 2024), tissue engineering (Saravanakumar et al., 2022; Liu et al., 2004), drug release (Huang & Huang, 2018; Vasi et al., 2014), cancer treatment (Kim, Moon, Kim, Heo, & Jeong, 2018; Hou, 2022) and bone regeneration (Zhai et al., 2020). Interestingly, depending on its molecular weight, it plays other physiological roles in processes such as wound healing and biosignaling (Serra, Casas, Toubarro, Barros, & Teixeira, 2023).

Despite several advantageous properties, one of the main limits of HA is its short half-life, as it lasts only a few days in the body because of rapid degradation through the action of hyaluronidases, a class of enzymes naturally present in the skin (Saturnino, 2014). In addition, the mechanical properties of unmodified hyaluronic acid are not suitable for applications such as dermal fillers or tissue engineering implants, that requires a more solid-like behaviour (Saravanakumar et al., 2022). For these reasons, HA-chemical modification strategies have been developed to improve its half-life and its physical and mechanical properties

E-mail addresses: elisa.martinelli@unipi.it (E. Martinelli), nicola.zerbinati@uninsubria.it (N. Zerbinati).

^a Department of Chemistry and Industrial Chemistry, University of Pisa, Pisa, Italy

b UB-CARE S.r.l. Spin-Off University of Pavia, Pavia, Italy

^c Department of Medicine and Technology Innovation, University of Insubria, Varese, Italy

^{*} Corresponding authors.

(Tiwari & Bahadur, 2019; Alonci et al., 2021; Faivre et al., 2021; Bokatyi, Dubashynskaya, & Skorik, 2024).

Ideally, a filler should be long-lasting, resorbable, not immunogenic, have minimal side effects, be easily injectable, and be cost-effective (De Boulle et al., 2013). The choice of the cross-linker is a crucial factor because it should be convenient for industrial processes, improve gel properties without impacting the biocompatibility and ensure long stability of the implant. Indeed, one of the main function of HA is to bind the receptor CD44 with carboxyl and hydroxyl function, so it is important to find an equilibrium between the improvement of gel properties and its biocompatibility, because a too high cross-linking density is known to reduce the availability of the carboxylic and hydroxyl function, inhibiting the HA ability of binding the receptor CD44, causing a decrease in biocompatibility and bioactivity (Santos, Paulino, & Brito Da Cruz, 2023; Øvrebø et al., 2024). 1,4-butanediol diglycidyl ether (BDDE) has historically been the most widely used cross-linker in HA-based commercial products (Faivre et al., 2021; Papakonstantinou, Roth, & Karakiulakis, 2012; Saturnino, 2014; Yang et al., 2016). In recent years, poly(ethylene glycol) diglycidyl ether (PEGDE) has been introduced as a promising alternative to BDDE for the development of HA-based dermal fillers (Faivre et al., 2021; Serra, Casas, Toubarro, Barros, & Teixeira, 2023Tang, Yu, Mondal, & Lin, 2023, Zerbinati et al., 2020, Santos et al., 2023) because of its interesting rheological properties and safety profile (Kim, 2025). A recent study has been reported on the comparison between HA-PEGDE and HA-BDDE hydrogels, observing higher cell viability for HA-PEGDE compared with HA-BDDE, in addition to a similar stiffness, despite the former formulation having a lower cross-linking density (Øvrebø et al., 2024).

The understanding of the relationship between the cross-linker structure and length, the physicochemical and mechanical properties, and the morphology of the corresponding hydrogel is extremely important (Faivre et al., 2021; Tang, Yu, Mondal, & Lin, 2023). However, such structure-properties relationship is not yet deeply understood (Øvrebø et al., 2024; Kim et al., 2023), even though it has been demonstrated that hydrogels with different mechanical properties interact differently with their surrounding biological environments and that the mechanical properties influence cell behaviour and stem cell differentiation (Xue, 2021; Ma, 2018; Xiang, 2022; Aldana, Valente, Dilley, & Doyle, 2021).

Considering the potential of PEGDE as cross-linker for HA hydrogels and the lack of a comprehensive structure-property study about the influence of the cross-linker length on hydrogel properties, in this work we synthesized PEGDE oligomers with well-defined lengths and used them as cross-linkers for different HA-based formulations, using polydisperse PEGDE as reference, too. The effect of the cross-linker length was studied by evaluating, for each formulation, the total PEGDE content, the molar amount of PEGDE that effectively acts as cross-linker, the thermal and rheological properties, solvent uptake kinetics, cross-linking density.

2. Results and discussion

2.1. Cross-linkers synthesis

Oligomers with well-defined lengths (degree of polymerization (n) from 2 to 6) along with a polydisperse PEGDE were synthesized through a $S_{\rm N}2$ reaction between mono- and poly-disperse poly(ethylene) glycols

(PEG) and epichlorohydrin (1) (Scheme 1). The reaction requires mild conditions, using NaOH pellets, and the products can be isolated after a simple filtration and removal of volatile compounds, followed by flash chromatography purification for monodisperse oligomers. The low yields associated with 2 and 3, composed of 2 and 3 repeating units, respectively, are due to their tendency to form polymerization byproducts (SI, Figure S1), identified by HPLC-Q-ToF analysis and removed by chromatographic purification.

The final products 2–7 were characterized by 1H NMR spectroscopy. Moreover, the 1H experiment was useful for the determination of the average number of repeating units in 7, which was found to be $n \sim 10$.

2.2. Hydrogel formulations

Products 2–7 and a commercial PEGDE (n $\sim 8)$ were used as cross-linkers of the HA matrix to obtain formulations 8–14, starting from the same HA/cross-linker molar ratio in the feed of 3 (n_{HA}/n_{cr-link}=3). The HA-based formulations were prepared modifying an already reported procedure for the synthesis of HA-BDDE hydrogels (Scheme 2) (Xue et al., 2020). Specifically, the preparation involved the dissolution of HA in a 0.5 M NaOH solution, followed by the addition of the cross-linker and incubation of the mixture, transferred into a capped jar, to obtain a gel disc, which was afterwards neutralized by the addition of 1 M HCl solution. PBS (pH = 7) was added to reach a final physiologically accepted HA concentration of 25 mg/mL. The gels were homogenized, transferred into syringes, and sterilized in an autoclave at 121 °C for 11 min to obtain a series of final cross-linked formulations that differ in the length and polydispersity of the cross-linker.

Moreover, a formulation containing BDDE as cross-linker (15), was also prepared as a reference sample under the same experimental conditions. The final products were suitable for a complete structure-property relationship study for understating the effect of the cross-linker chain length and polydispersity on both chemical and rheological properties.

2.3. Chemical characterization

2.3.1. Total PEGDE content determination by ¹H NMR

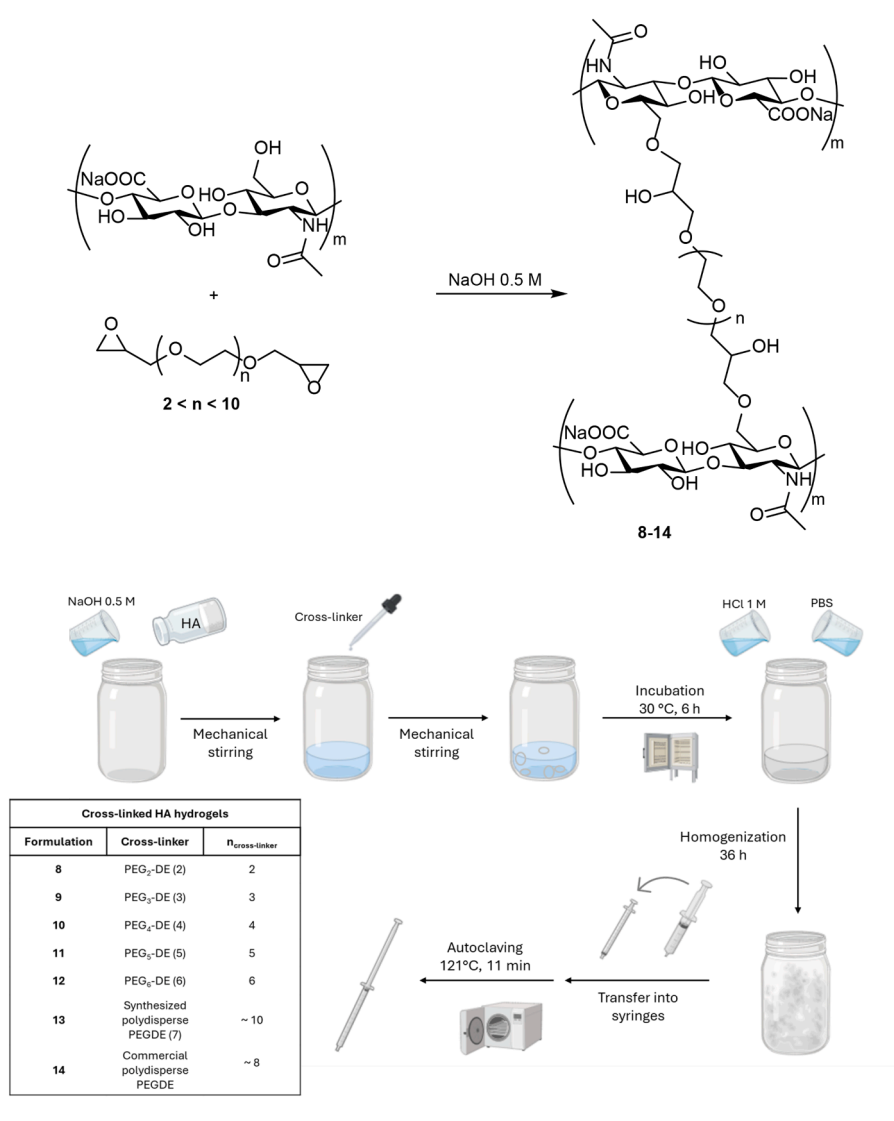
The total molar amount of PEGDE cross-linker (Tot_{cr-link}) in the formulations was estimated by 1H NMR experiments in D₂O after the degradation of the samples by an acidic digestion (0.2 M HCl at 60 $^{\circ}$ C). In particular, the signal at 2.0 ppm corresponding to the acetamide methyl group and the signals at 3.1 - 4.0 ppm due to both PEGDE protons and 10 protons of the hyaluronic acid backbone (Fig. 1) were used for the calculation of the Tot_{cr-link}, according to the equations reported in the Experimental section.

Interestingly, although the HA/cross-linker molar ratio in the feed was the same for all the investigated formulations, the $Tot_{cr-link}$ value was found to decrease from 16 % to 8.2 % by increasing the PEGDE length from 2 to \sim 10 units (SI, Figure S2), thus suggesting that shorter cross-linkers are more reactive than longer ones, as a result of their lower molecular weight and higher availability of the reactive functional groups. The ^1H NMR signals of mono- and cross-linked chains fall in the same region, thus preventing the discrimination between the two species and the estimation of the effective molar amount of PEDGE that acts as cross-linker by reacting at both sides.

For the HA-BDDE formulation (15) a $Tot_{cr\text{-link}}$ of 13 % was calculated

HO
$$\begin{pmatrix} 1 \\ 1 \\ 1 \end{pmatrix}$$
 $\begin{pmatrix} 1 \\ 1 \\ 1 \end{pmatrix}$ $\begin{pmatrix} 1 \\ 1 \\ 1 \end{pmatrix}$ $\begin{pmatrix} 1 \\ 1 \\ 1 \end{pmatrix}$ $\begin{pmatrix} 1 \\ 1 \\ 2 \end{pmatrix}$ $\begin{pmatrix} 1 \\ 1 \\ 2 \end{pmatrix}$ $\begin{pmatrix} 1 \\ 1 \\ 3 \end{pmatrix}$ $\begin{pmatrix} 1 \\ 1 \\ 1 \end{pmatrix}$ $\begin{pmatrix} 1 \\ 1 \\ 3 \end{pmatrix}$ $\begin{pmatrix} 1 \\ 1 \\$

Scheme 1. Optimized conditions for the synthesis of PEGDE-based cross-linkers with different lengths.



Scheme 2. Reaction scheme for the synthesis of cross-linked HA (top) and schematic illustration of the procedure for the preparation of the HA cross-linked hydrogels (bottom).

by considering the 1 H NMR signals at 2.0 and 1.5 ppm corresponding to the methyl group of the HA acetamide and the CH₂CH₂ protons of the cross-linker, respectively. This value is lower than that obtained for the formulation 8 containing the PEGDE with n = 2, i.e., the same number of carbon atoms as BDDE, and equal to that obtained for formulation 10 based on a PEGDE with n = 4, that is twice as many carbon atoms as BDDE (Bang, Das, Yu, & Noh, 2017).

2.3.2. Thermal analysis

PEGDE cross-linkers and HA-based formulations were subjected to thermal characterization to preliminarily evaluate their thermal stability (SI, Figure S3 and S4), especially in view of their resistance toward steam sterilization. All the PEGDE cross-linkers showed similar TGA curves with a first small degradation step below 100 °C, due to the release of absorbed moisture, and a second degradation step characterized by a Tonset in the range 175–193 °C and a Tmax in the range 204–235 °C, progressively increasing with the length of the PEGDE from n=2 to ~ 8 (Table 1). The final residue at 700 °C was almost zero for all the oligomers.

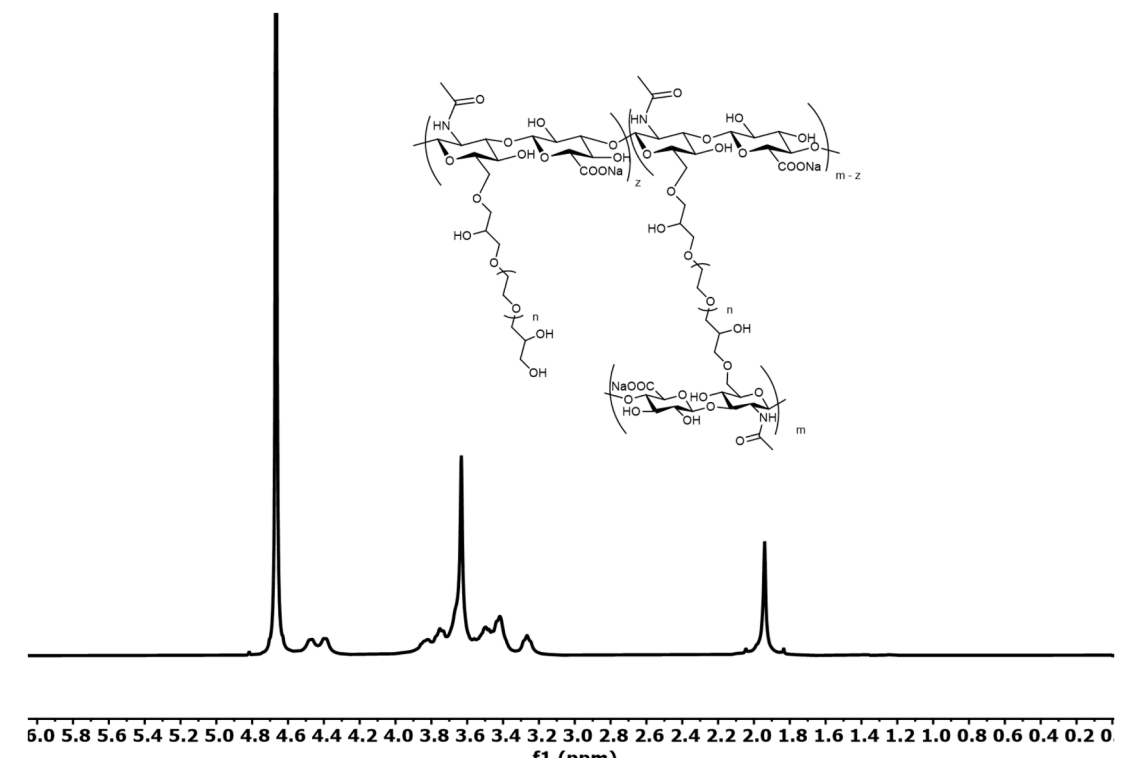
HA-based formulations showed a first mass loss of almost 10 wt % below 100 °C due to the moisture evaporation, and a main mass loss in the range 230–400 °C. Such TGA profiles agree with what was previously reported in the literature for analogue HA-BDDE gels and are

associated with the decomposition of HA, cross-liker chains, and complete breakdown of cross-linked network (Bang, Das, Yu, & Noh, 2017). $T_{\rm onset}$, $T_{\rm max}$ and mass loss % of the main degradation step together with the residue at 700 °C for all the dry samples (rescaled for the moisture evaporation) are reported in Table 2. The degradation steps of the cross-linkers are not present in the TGA curve of the corresponding HA based formulation. The main degradation step of HA moves to lower temperatures and the residues at 700 °C of the HA based formulations are higher than that of HA.

These data confirm the covalent anchorage of the cross-linker to HA and the formation of a thermostable fraction increasing the residue at 700 $^{\circ}\text{C}$ with respect to the pure HA. On the other hand, the gels are slightly less thermostable than pure HA, maybe due to the lower thermostability of the cross-linker compared to HA.

2.4. Rheology

Across the studies reported in the literature, many factors influence the hydrogel viscoelastic properties, such as HA concentration, molecular weight, cross-linking technology, free HA amount, and cross-linker (Wongprasert, Dreiss, & Murray, 2022). Cross-linked hyaluronic acid hydrogels behave as viscoelastic solids, *i.e.*, they exhibit both viscous and elastic behavior, the latter being predominant. The most important



f1 (ppm) Fig. 1. ¹H NMR spectrum in D₂O of the HA-based hydrogel after acid degradation.

Table 1 T_{onset} , and T_{max} of the main degradation step of PEGDE cross-linkers.

Council T (CO) T	(0.0)
Sample n T_{onset} (°C) T_{max}	x (°C)
3 3 175 204	
4 4 193 218	i
5 5 192 217	
6 6 179 217	
Commercial PEGDE ~ 8 193 235	

Table 2 T_{onset} , T_{max} mass loss % of the main degradation step and the residue at 700 °C of HA and HA-based formulations.

Sample	n	T _{onset} (°C)	T _{max} /mass loss (°C/%m/m)	Residue (700°C)
8	2	233	255/64 %	36 %
9	3	232	251/59 %	41 %
10	4	233	248/57 %	42 %
11	5	233	246/57 %	42 %
12	6	234	255/60 %	40 %
14	~ 8	236	248/61 %	39 %

parameters used to describe the rheological behavior of a hydrogel are the storage modulus (G'), the loss modulus (G''), the tangent phase angle ($\tan \delta$), and the complex modulus (G*). If G' is higher than G'' ($\tan \delta < 1$), as usual for cross-linked hydrogels, then the gel is firmer, with a more elastic response to shear deformation. If G'' is higher than G' ($\tan \delta > 1$), the material is softer and liquid-like, for example non-cross-linked HA solutions (Fundarò, Salti, Malgapo, & Innocenti, 2022). These rheological parameters can be used to understand the behavior of a gel when subjected to the conditions and mechanical forces of its medical use, such as during injection through a thin needle into the skin (Zerbinati et al., 2021b).

Amplitude sweep consists in applying an increasing shear stress on the material at a fixed frequency and allows the determination of the linear viscoelastic region (LVER), *i.e.*, the conditions in which the applied stress is insufficient to cause the structural breakdown (yielding) of the material. After the end of the LVER, in most hydrogels, the material response is not linear, and a crossover point is often observed (G' becomes equal and then lower than G'').

Given the importance of the rheological properties for the performance and biocompatibility of an hydrogel, the behavior of HA-based formulations was studied (Tezel & Fredrickson, 2008). Results obtained for the amplitude sweep experiments are collected in Table 3, with reference to the values of G, G, G, and δ taken at 1 % strain. The end of the LVER is also reported.

For all the investigated samples, G was higher than G (Table 3 and SI, Section 4.1) and it increased from 52.0 to 114.7 Pa, by increasing the cross-linker chain length from n=2 to n=6. For higher values of n it appear to reach a *plateau* (Fig. 2). The statistical significance was assessed by comparing each formulation (8–14) with the others (SI, Table S17), observing a meaningful statistical significance between formulations with n < 5 and those with n > 5. Sample 13, containing the

Table 3 Rheological characterization of HA-based hydrogels at 12 $^{\circ}$ C. Each sample was analyzed in triplicate.

Sample	G' (Pa)	G" (Pa)	tan δ	G* (Pa)	End of LVER (%)
8	52.0 ± 5.9	$\begin{array}{c} \textbf{22.3} \pm \\ \textbf{2.4} \end{array}$	$\begin{array}{c} \textbf{0.429} \pm \\ \textbf{0.005} \end{array}$	56.5 ± 6.3	17.86 ± 2.05
9	$64.7 \pm \\13.3$	$\begin{array}{c} \textbf{23.9} \pm \\ \textbf{5.1} \end{array}$	$\begin{array}{c} 0.369 \pm \\ 0.010 \end{array}$	$68.9 \pm \\14.2$	16.88 ± 4.90
10	$\textbf{77.2} \pm \textbf{4.9}$	$\begin{array}{c} \textbf{22.7} \ \pm \\ \textbf{1.7} \end{array}$	0.294 ± 0.005	80.4 ± 5.1	20.04 ± 2.31
11	90.5 ± 8.0	$\begin{array}{c} 25.2 \pm \\ 3.0 \end{array}$	0.279 ± 0.019	94.0 ± 8.4	18.82 ± 4.24
12	$\begin{array}{c} 114.7 \; \pm \\ 15.0 \end{array}$	$\begin{array}{c} \textbf{22.8} \pm \\ \textbf{3.4} \end{array}$	0.199 ± 0.018	$117.0 \pm \\15.2$	17.78 ± 0.01
13	$110.5 \pm \\3.4$	$\begin{array}{c} \textbf{24.0} \; \pm \\ \textbf{2.0} \end{array}$	$\begin{array}{c} \textbf{0.217} \pm \\ \textbf{0.020} \end{array}$	$\begin{array}{c} 113.0 \pm \\ 3.3 \end{array}$	16.05 ± 3.00
14	$\begin{array}{c} \textbf{110.4} \pm \\ \textbf{8.1} \end{array}$	$\begin{array}{c} 21.6 \; \pm \\ 2.2 \end{array}$	$\begin{array}{c} \textbf{0.197} \pm \\ \textbf{0.023} \end{array}$	$\begin{array}{c} 112.5 \pm \\ 8.0 \end{array}$	16.49 ± 1.12

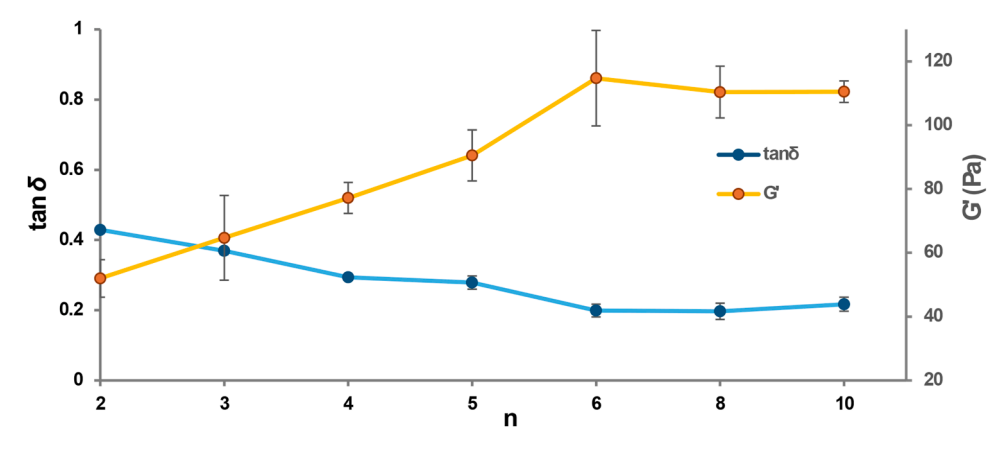


Fig. 2. Values of tan δ as a function of the cross-linker length.

synthetic PEGDE with $n \sim 10$ possessed rheological properties similar to sample 14, prepared by using the commercially available PEGDE with n \sim 8. All the samples displayed a similar LVER, ranging in between 15 % and 20 %. Such behavior is also typical of analogue HA-based hydrogels (Zerbinati et al., 2021a; Zerbinati et al., 2021b; Zerbinati et al., 2022). In Fig. 2, the values of tan δ as a function of the cross-linker length are reported. Generally, for hydrogel formulations containing a given cross-linker, tan δ is usually associated with the cross-linking density, with lower values for highly cross-linked hydrogels than for less cross-linked ones (Fundarò, Salti, Malgapo, & Innocenti, 2022). However, for the present hydrogel formulations, which differ for the incorporated cross-linker, a variation in $\tan\delta$ can be attributed to differences in cross-linking density as well as to the length of the cross-linker or a combination of the two parameters. In general, the values observed for G' and tan δ are comparable with those obtained for commercial HA-PEGDE hydrogels (Tang, Yu, Mondal, & Lin, 2023).

To have a better comprehension of this trend in rheological behavior, solvent-uptake measurements were carried out to evaluate the cross-linking density of the hydrogel formulations.

To further evaluate the rheological behavior of the material, a frequency sweep test was carried out with the aim of predicting the dermal filler behavior when subjected to periodic stress and deformation caused by the physiological movement of muscles and tissues. The frequency range 0.1–2 Hz is physiologically relevant for skin and facial indications, so the results obtained are extrapolated at 1 Hz (Zerbinati et al., 2022; Winkler, Lorenc, Öhrlund, & Phd, 2017). All the samples analyzed showed a similar behavior, with *G*' and *G*" running almost parallel with a positive slope (SI, Section 4.2). No crossover point was observed at all

frequencies investigated, indicating that the elastic nature of the gel prevailed on the viscous one, as is typical for cross-linked hydrogel materials.

2.5. Solvent-uptake kinetics

The ability of a gel to absorb a good solvent is generally correlated to the cross-linking density or degree: more cross-linked gels absorb less solvent than less cross-linked ones (Lange, 1986). For this reason, solvent-uptake measurements were performed to gain qualitative information about the different cross-linking densities of the HA-based formulations, through the determination of a kinetic curve of the solvent uptake. Water is a very good solvent for HA-PEGDE hydrogels (Øvrebø et al., 2024), but its absorption quickly causes the rupture of the material, thus preventing the absorption kinetics study. Therefore, methanol was selected as an alternative polar solvent, capable of swelling the gel, without causing its rupture for the entire period of the measurement (30 min). In particular, for all the investigated formulations a plateau in the value of the solvent-uptake was reached after 10 min (Fig. 3). Interestingly, the methanol uptake generally increases by increasing the length (n) of the cross-linker (SI, Section 5) indicating that HA-based gels with longer PEGDEs are less cross-linked.

However, by taking advantage of the solvent-uptake measurements, it is possible to calculate the cross-linking density (ν) by the Flory-Rehner Eq. (1):

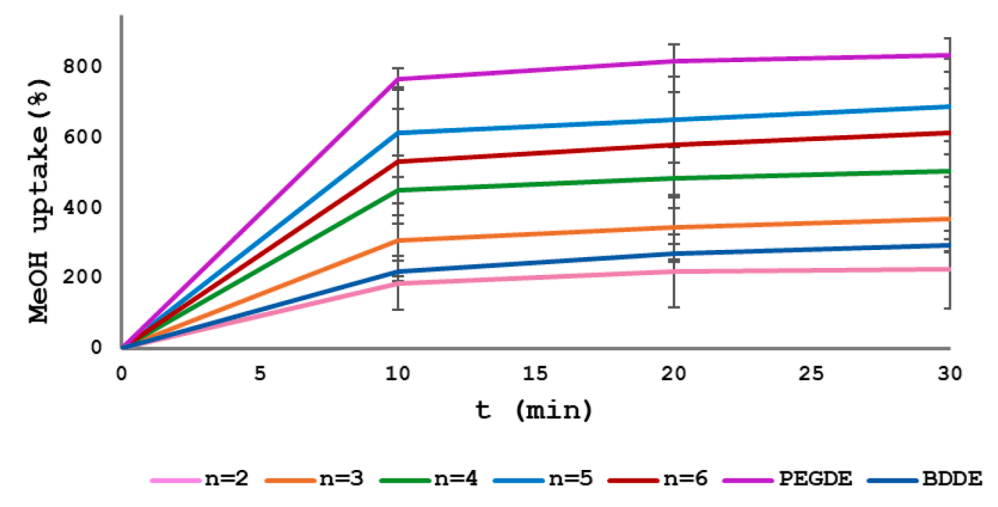


Fig. 3. Methanol uptake as a function of immersion time for formulations 8–12, 14 and 15.

$$\nu = \frac{d}{M_{\rm c}} = -\frac{\ln(1-\phi_{\rm p}) + \phi_{\rm p} + \chi \phi_{\rm p}^2}{V_{\rm s} \left(\phi_{\rm p}^{\frac{1}{3}} - \frac{1}{2}\phi_{\rm p}\right)}$$
(1)

where d is the density of the polymer, M_c is the average molar mass of the polymer chain between two adjacent cross-linking points, ϕ_p is the polymer volume fraction in the swollen state, χ is the Flory-Huggins polymer-solvent interaction parameter and V_s is the molar volume of the solvent. Although the χ parameter is tabulated for many polymersolvent pairs (Winkler, Lorenc, Öhrlund, & Phd, 2017), this is not the case for HA-MeOH pair. Thus, it was necessary to calculate γ according to Eq. (2) (where R = 8.314 J/(mol K) is the universal gas constant and T (K) is the absolute temperature), which requires using solubility parameters. Since the latter values are also not reported in the literature for the HA-MeOH pair, they were determined by the group contribution method of Hoftyzer-Van Krevelen (Table 4, Krevelen & Te Nijenhuis, 2009) according to Eq. (3), where V is the molar volume of HA (308.64 cm³/mol), calculated as the ratio between the average molecular weight of HA repeating unit (379.32 g/mol) and the density of HA powder (1.229 g/cm³) (Van-Krevelen & Te Nijenhuis, 2009).

$$\chi = \frac{V_s \left[\left(\delta_{dS} - \delta_{dP} \right)^2 + 0.25 \left(\delta_{pS} - \delta_{pP} \right)^2 + 0.25 \left(\delta_{hS} - \delta_{hP} \right)^2 \right]}{RT} \tag{2} \label{eq:eqn:equation_problem}$$

$$\delta_{d} = \frac{\sum F_{di}}{V} \ \delta_{p} = \frac{\sqrt{\sum F_{pi}^{2}}}{V} \ \delta_{h} = \sqrt{\frac{\sum E_{hi}}{V}} \ \ensuremath{ (3)} \label{eq:delta_delta_delta}$$

The calculated solubility parameters for HA are $\delta_d=13.3~(\mathrm{J/cm^3})^{1/2},$ $\delta_p=5.1~(\mathrm{J/cm^3})^{1/2},$ $\delta_h=18.6~(\mathrm{J/cm^3})^{1/2}.$ On the other hand, the values of δ_d , δ_p , δ_h and V_s for MeOH are tabulated and correspond to 15.1, 12.3, and 22.3 $(\mathrm{J/cm^3})^{1/2}$, and 40.7 $\mathrm{g/cm^3}$, respectively (Krevelen & Te Nijenhuis, 2009). Given δ_d , δ_p , and δ_h for both the polymer (P) and the solvent (S), the Flory-Huggins parameter for the HA-MeOH pair was calculated to be 0.32 according to Eq. (2).

Such a value was then included in the Flory-Rehner Eq. (1), where $\phi_{\rm p}$ was determined experimentally by the solvent-uptake measurements, d = 1.229 g/cm³ and $V_s = 40.7$ cm³/mol. In agreement with the formulation composition and solvent uptake results, formulations with a shorter PEGDE cross-linker was generally characterized by higher values of cross-linking density (ν) (Table 5), indicating they were more crosslinked. Moreover, the molar fraction of HA units that were crosslinked (x_{HAcr-link}) in the various formulations was calculated starting from the value of ν , the density of the polymer, and the average molecular weight of the repeating unit. The calculated $x_{\text{HAcr-link}} \, \text{decreased}$ from 11 mol % to 2 mol % by increasing the length of the PEGDE from 2 to \sim 8 (for commercial polydisperse PEGDE). Based on the total content of PEDGE cross-linker in the formulation (Tot_{cr-link}), it was also possible to determine the molar amount of PEGDE effectively involved in the formation of cross-linking points at both sides (Cr_{PEGDE}). Cr_{PEGDE} values decreased from 70 mol % to 26 mol % by increasing the PEGDE length from 2 to ~ 8. These values were generally higher than that evaluated

$$\label{eq:table 4} \begin{split} &F_{di},F_{pi}^2 \text{ and } E_{hi} \text{ values for each group of the repeating unit of HA calculated by the} \\ &Hoftyzer-Van \text{ Krevelen method for the calculation of solubility parameters.} \end{split}$$

Group n°		$F_{di} (Jcm^3/mol)^{1/2}$	F _{pi} (Jcm ³ /mol)	E _{hi} (J/mol)	
CH ₃	1	420	0	0	
CH ₂	1	270	0	0	
CH	10	800	0	0	
ОН	4	840	1000,000	80,000	
O	4	400	640,000	12,000	
СООН	1	530	176,400	10,000	
NH	1	160	44,100	3100	
CO	1	290	592,900	2000	
Ring	2	380	_	_	
TOTAL		4090	2453,400	107,100	

Table 5 Cross-linking density (ν), molar percentage of HA repeating units that are cross-linked in the formulation ($x_{\rm HAcross-link}$) and molar percentage of PEGDE that effectively acts as crosslinker in the formulation ($Cr_{\rm PEGDE}$).

Sample	m (mg) t = 0 min	m (mg) t = 30 min	ν (mmol/ cm ³)	M _c (g/ mol)	x _{HAcross-link} (mol %)	Cr _{PEGDE} (mol%)
8	60.2	252.3	0.36	3398	11	70
9	53.2	248.1	0.28	4320	9	61
10	54.9	326.9	0.17	7301	5	40
11	48.7	421.2	0.08	15,499	2	20
12	77.0	550.8	0.12	10,634	3	31
14	73.0	679.5	0.07	17,879	2	26
15	62.1	244.2	0.42	2934	13	81

from ¹³C NMR spectroscopy for similar HA-based hydrogels (Monticelli et al., 2019). Findings obtained for solvent uptake, cross-linking density, x_{HAcross-link} and Cr_{PEGDE} are all consistent in supporting that formulations containing longer PEGDEs are less cross-linked. On the other hand, they are stiffer, as proven by the lower values of tan δ and higher values of G'. A similar behaviour although unexpected and not yet fully understood, has already been described in literature for HA-PEGDE (comparable to sample 14 of this work) and HA-BDDE hydrogels (Øvrebø et al., 2024). In particular, the authors reported that HA-PEGDE gels exhibited comparable stiffness with respect to HA-BDDE, despite a lower effective crosslinking ratio, that is a lower cross-linking density. Therefore, our study consistently highlights the pivotal role of the type of the cross-linker, rather than the cross-linking density, in determining the rheological behavior of the HA-based. Such a behavior suggests that the length and flexibility of PEGDE chain influence the rheological properties of the gel more than relatively slight changes in cross-linking density. Finally, we can speculate that among all the investigated formulations the one containing the longest polydisperse PEGDE is preferred for the envisaged application, as it combines superior rheological performance with a lower cross-linker density. The latter aspect is of particular biological relevance since high cross-linking densities are known to limit the HA ability to bind the CD44 ligand, that results in a reduction of its biocompatibility.

3. Experimental section

3.1. Materials and methods

Di-, tri-, tetra-, and pentaethylene glycol and epichlorohydrin were purchased from Thermo Scientific. Hexaethylene glycol, PEG400 and PEGDE were purchased from TCI, VWR and BocSciences, respectively. Hyaluronic acid was bought by Contipro. All the reagents were used as received.

The cross-linker synthesis was monitored by HPLC-Q-ToF (1260 Infinity II HPLC + 6530 LC/Q-TOF, Agilent Technologies) and thin-layer chromatography using Merck silica gel 60 F254 plates. The chromatogram developed was visualized by aqueous potassium permanganate. Flash chromatography was performed by using Sigma-Aldrich silica gel 60, particle size $40-63~\mu m$, with the indicated solvent system. $^1 H$ NMR spectra of cross-linkers were registered with $^1 H$ NMR on a Jeol instrument JNM-ECZ400R or JNM-ECZ500R. Chemical shifts are reported in ppm with the deuterated solvent signal as the internal standard. Data are reported as follows: chemical shift, integration, multiplicity (s = singlet, d = doublet, t = triplet, q = quartet, qn = quintet, m = multiplet, and br = broad), with the coupling constant in hertz.

3.1.1. General method A: Synthesis of the cross-linkers 2-7

Mono- or polydisperse poly(ethylene) glycol (1 equiv.), NaOH (5 equiv.) and $\rm H_2O$ (1.33 equiv.) were added to a two-necked round-bottomed flask equipped with a refrigerator and left to stir for 10 min before adding epichlorohydrin (6 equiv.) drop by drop. The mixture was

stirred at 45 °C for 3 h, then diluted with DCM and filtered. The filtrate was washed with DCM and the solution was dried over Na₂SO₄. The solvent was removed under reduced pressure to give the crude product. The monodisperse oligomers were purified by flash chromatography.

3.1.2. Hydrogel formulation (8-15)

Hyaluronic acid was dissolved in a 0.5 M NaOH solution to obtain an initial concentration of 112 mg/mL. The cross-linker was added so that the molar ratio $n_{\rm HA}/n_{\rm cr-link}$ was 3. The obtained mixture was stirred under mechanical stirring. The mixture was transferred into a capped jar and incubated at 40 °C for 6 h in a TCN50 Plus, Argo Lab oven to obtain a gel disc that was neutralized by adding a 1 M HCl solution. PBS (pH = 7) was added to reach a final HA concentration of 25 mg/mL. The gel was homogenized and transferred into 1 mL syringes, which were sterilized at 121 °C for 11 min in an autoclave (DX-45, Systec).

3.1.3. ¹H NMR experiment

The 1H NMR experiment was performed on degraded hydrogels. The formulation was washed first with MeCN:H₂O 95:5 and then with MeCN, to remove the residual cross-linker. The gel was dried under reduced pressure at 60 $^{\circ}C$ and the residue was degraded with 3 mL of 0.2 M HCl solution at 60 $^{\circ}C$ for 2 h. The mixture was neutralized by adding a 0.4 M NaOH solution and PBS. The final solution was dried under reduced pressure at 60 $^{\circ}C$. The residue was dissolved in D₂O. ^{1}H NMR experiments were recorded using 64 scans and a relaxation delay of 5 s. The total molar amount of PEGDE cross-linker (Tot_{cr-link}) in the final formulations was calculated by considering the signal at 2.0 ppm due to -CH₃CONH and the signals at 3.1–4.0 ppm associated with both -CH₂CH₂O- of PEG and 10 protons of the hyaluronic acid backbone, according to Eq. (4):

$$\mathbf{Tot}_{\mathbf{cr-link}} (\%) = \frac{\frac{\frac{1^{53.1-4.0pm}}{\text{corrected}}}{n_{\text{H}_{\text{cross-linker}}}}}{\frac{1^{62.0ppm}}{3} + \frac{\frac{1^{63.1-4.0ppm}}{\text{corrected}}}{n_{\text{H}_{\text{pross-linker}}}}}$$

$$(4)$$

where $I_{corrected}^{\delta 3.1-4.0ppm}$ is the integral of the region at 3.1-4.0 ppm subtracted by 10 protons of hyaluronic acid present in the same range of chemical shifts and $I^{\delta 2.0ppm}$ is the integral of the peak at 2.0 ppm of the three protons of the methyl group on the N-acetylglucosamine residue. $n_{H_{cross-linker}}$ is the total number of protons in the PEGDE of length n ($n_{H_{cross-linker}}$ = n_{*} 4 $_{+10}$).

3.1.4. Thermal stability

TGA experiments were carried out with a Perkin Elmer TGA 8000 instrument. Measurements were performed at a rate of 10 $^{\circ}$ C/min, from 30 $^{\circ}$ C to 700 $^{\circ}$ C under nitrogen flow (25 mL/min). The amount of sample in each TGA measurement varied between 2 and 4 mg.

3.1.5. Amplitude sweep test for linear viscoelastic region (LVER) determination

An internal amplitude sweep test sequence was set to determine the linear viscoelastic region (LVER), where it was possible to work on the samples without damaging their inner structure, and the G'-G'' crossover point, which represents the transition from solid-like to liquid-like behavior determined by $\tan\delta=1$. In LVER, G', G''and $\tan\delta$ should be constant at increasing shear strain. The following parameters were set: temperature of 25 °C, frequency 1 Hz, 5 points per decade from 0.01 to 1 %, 20 points per decade between 1 and 100 % and 30 points per decade in the range 100–1000 %. Analyses were performed in triplicate. The data processing was performed with rSpace for Kinexus software (Malvern Panalytical, Worcestershire, UK).

3.1.6. Frequency sweep test

0.2 g of sample were loaded between the two rigid geometries, with a 1 mm gap, the superior oscillates at a constant shear strain (1 %), chosen

in the LVER to avoid permanent damage to the internal structure, while the lower is heated at a fixed temperature of 25 $^{\circ}$ C. The frequency range tested is between 0.1 and 10 Hz with 10 points per decade. Each analysis was performed in triplicate. Rheological analyses were performed by using Kinexus Plus Rheometer (Malvern Panalytical, Worcestershire, UK) while data processing was performed using rSpace for Kinexus software version 1.76 (Malvern Panalytical).

3.1.7. Solvent-uptake kinetics

The hydrogel was lyophilized overnight, and the dry sample was weighed (w_{dry}). Then the dry sample was immersed in MeOH and weighed after 10, 20, and 30 min of immersion (w_{wet}). Each sample was analyzed in triplicate. The percentage of solvent-uptake was calculated according to the Eq. (5):

$$MeOH \ uptake = \frac{w_{wet} - w_{dry}}{w_{dry}} * 100$$
 (5)

3.1.8. Statistical analysis of G'

To evaluate the statistical significance, each formulation (8–14) was analyzed compared to the others. Values of 0.12 (ns), 0.033 (*), 0.002 (**) and <0.001 (***) were considered statistically significant using Graphpad Prism 10.5.0. (774) One-way ANOVA analysis. Šidák's statistical hypotheses test correction was used for multiple comparisons. The multiplicity was the adjusted P value for each comparison with a 95 % confidence interval.

4. Conclusion

In the current work PEGDE of different lengths were synthesized and used as cross-linkers of hyaluronic acid. Despite starting from the same cross-linker/HA mole ratio in the feed, the molar amount of PEGDE, the cross-linking density and rheological properties of the prepared hydrogels were found to strongly depend on the length of the PEGDE crosslinker. In particular, the total and effective molar amount of PEGDE cross-linker in the formulation as well as the cross-linking density decreased as the cross-linker length increased. Specifically, the total amount and effective amount of PEGDE cross-linker decreases from 16.0 % to 9.9 % and from 70 mol % to 26 mol %, respectively by increasing the PEGDE length from 2 to ~ 8 units. On the other hand, hydrogels containing the longer PEGDEs were generally stiffer (G' value increased from 52.0 to 114.7 Pa by increasing the cross-linker chain length, before reaching a plateau at n = 6), despite having a lower total and effective molar amount of PEGDE cross-linker and a lower cross-linking density. Overall, these results highlight the pivotal role of the cross-linker length in determining the properties of HA-based hydrogels and suggest that its design has to be carefully controlled when engineering an HA-based material for biomedical applications.

CRediT authorship contribution statement

Fabiana Cordella: Writing – original draft, Methodology, Investigation, Data curation, Conceptualization. Giuseppe Alonci: Writing – review & editing, Supervision, Methodology, Conceptualization. Gaetano Angelici: Writing – review & editing, Supervision, Methodology, Funding acquisition, Conceptualization. Roberto Mocchi: Writing – review & editing, Visualization. Martina Savona: Methodology, Investigation. Giulia Grimaldi: Methodology, Investigation. Giulia Galasso: Investigation. Sabrina Sommatis: Visualization. Celia Duce: Writing – original draft, Methodology. Elena Pulidori: Writing – original draft, Investigation. Elisa Martinelli: Writing – review & editing, Supervision, Methodology, Data curation, Conceptualization. Nicola Zerbinati: Writing – review & editing, Visualization, Supervision, Funding acquisition.

Declaration of competing interest

The authors declare that they have no known competing financial interests or personal relationships that could have appeared to influence the work reported in this paper.

Acknowledgements

FC acknowledges financial support from Matex Lab Switzerland S.A. and from the FSE-REACT-EU programme, PON "Ricerca e Innovazione" 2014–2020 (D.M. 1061/2021) Azione IV.5 "Dottorati su tematiche Green".

Supplementary materials

Supplementary material associated with this article can be found, in the online version, at doi:10.1016/j.carpta.2025.100908.

Data availability

Data will be made available on request.

References

- Aldana, A. A., Valente, F., Dilley, R., & Doyle, B. (2021). Development of 3D bioprinted GelMA-alginate hydrogels with tunable mechanical properties. *Bioprinting*, 21, Article e00105.
- Al-Halaseh, L. K., et al. (2022). A review of the cosmetic use and potentially therapeutic importance of hyaluronic acid. *Journal of Applied Pharmaceutical Science*, 12, 34–41.
- Alonci, G., et al. (2021). Physico-chemical characterization and in vitro biological evaluation of a bionic hydrogel based on hyaluronic acid and L-lysine for medical applications. *Pharmaceutics*, 13,, 1194.
- Bang, S., Das, D., Yu, J., & Noh, I. (2017). Evaluation of MC3T3 cells proliferation and drug release study from sodium hyaluronate-1,4-butanediol diglycidyl ether patterned gel. *Nanomaterials*, 7(10), 328.
- Bokatyi, A. N., Dubashynskaya, N. V., & Skorik, Y. A. (2024). Chemical modification of hyaluronic acid as a strategy for the development of advanced drug delivery systems. *Carbohydrate Polymers*, 337, Article 122145.
- De Boulle, K., et al. (2013). A review of the metabolism of 1,4-butanediol diglycidyl ether-crosslinked hyaluronic acid dermal fillers. *Dermatologic Surgery*, 39, 1758–1766.
- Faivre, J., et al. (2021). Crosslinking hyaluronic acid soft-tissue fillers: current status and perspectives from an industrial point of view. Expert Review of Medical Devices, 18, 1175–1187.
- Fundarò, S. P., Salti, G., Malgapo, D. M. H., & Innocenti, S. (2022). The rheology and physicochemical characteristics of hyaluronic acid fillers: their clinical implications. *International Journal of Molecular Sciences*, 23(18), Article 10518.
- Hintze, V., Schnabelrauch, M., & Rother, S. (2022). Chemical modification of hyaluronan and their biomedical applications. Frontiers in Chemistry, 10, Article 830671.
- Hong, G. W., et al. (2024). Manufacturing process of hyaluronic acid dermal fillers. *Polymers (Basel)*. 16(19). Article 2739.
- Hou, X., et al. (2022). Recent advances in hyaluronic acid-based nanomedicines: preparation and application in cancer therapy. *Carbohydrate Polymers*, 292, Article 119662.
- Huang, G., & Huang, H. (2018). Application of hyaluronic acid as carriers in drug delivery. *Drug Delivery*, 25, 766–772.
- Huerta Ángeles, G., & Nesporová, K. (2021). Hyaluronan and its derivatives for ophthalmology: recent advances and future perspectives. *Carbohydrate Polymers*, 259. Article 117697.
- Kim, D. H., et al. (2025). Comparative toxicity study of hyaluronic acid fillers crosslinked with 1,4-butanediol diglycidyl ether or poly (ethylene glycol) diglycidyl ether. *International Journal of Biological Macromolecules*, 296, Article 139620.
- Kim, J. H., Moon, M. J., Kim, D. Y., Heo, S. H., & Jeong, Y. Y. (2018). Hyaluronic acid-based nanomaterials for cancer therapy. *Polymers (Basel)*, 10(10), 1133.
- Kim, M., et al. (2023). Effect of cross-linker chain length on biophysical property of hyaluronic acid hydrogel dermal filler. *Macromolecular Research*, *31*, 843–850.
- Krevelen, D. W. Van, & Te Nijenhuis, K. (2009). *Properties of Polymers* (pp. 189–225). Elsevier.

- Lange, H. (1986). Colloid & Polymer Science determination of the degree of swelling and crosslinking of extremely small polymer gel quantities by analytical ultracentrifugation. Colloid and Polymer Science, 24, Article 488493.
- Liu, H., et al. (2004). A study on a chitosan-gelatin-hyaluronic acid scaffold as artificial skin in vitro and its tissue engineering applications. *Journal of Biomaterials Science Polymer Edition*, 15, 25–40.
- Ma, Y., et al. (2018). 3D Spatiotemporal mechanical microenvironment: a hydrogelbased platform for guiding stem cell fate. Advanced Materials, 30(49), Article 1705911.
- Monticelli, D., et al. (2019). Chemical characterization of hydrogels crosslinked with polyethylene glycol for soft tissue augmentation. Open Access Macedonian Journal of Medical Sciences, 7, 1077–1081.
- Øvrebø, Ø., et al. (2024). Characterisation and biocompatibility of crosslinked hyaluronic acid with BDDE and PEGDE for clinical applications. *Reactive & Functional Polymers*, 200. Article 105920.
- Papakonstantinou, E., Roth, M., & Karakiulakis, G. (2012). Hyaluronic acid: a key molecule in skin aging. *Dermato-Endocrinology*, 4(3), 253–258.
- Santos, V., Paulino, P., & Brito Da Cruz, M. (2023). Hyaluronic acid aesthetic fillers: a review of rheological and physicochemical properties. Article in Journal of Cosmetic Science, 74(2), 132–142.
- Saravanakumar, K., et al. (2022). Application of hyaluronic acid in tissue engineering, regenerative medicine, and nanomedicine: a review. *International Journal of Biological Macromolecules*, 222, 2744–2760.
- Saturnino, C., et al. (2014). Acetylated hyaluronic acid: Enhanced bioavailability and biological studies. *BioMed Research International*, 2014, Article 921549.
- Schanté, C. E., Zuber, G., Herlin, C., & Vandamme, T. F. (2011). Chemical modifications of hyaluronic acid for the synthesis of derivatives for a broad range of biomedical applications. *Carbohydrate Polymers*, 85, 469–489.
- Serra, M., Casas, A., Toubarro, D., Barros, A. N., & Teixeira, J. A. (2023). Microbial hyaluronic acid production: a review. *Molecules*, 28(5), 2084.
- Tang, Z., Yu, M., Mondal, A. K., & Lin, X. (2023). Porous scaffolds based on polydopamine/chondroitin sulfate/polyvinyl alcohol composite hydrogels. *Polymers* (Basel), 15(2), 271.
- Tezel, A., & Fredrickson, G. H. (2008). The science of hyaluronic acid dermal fillers. Journal of Cosmetic and Laser Therapy, 10, 35–42.
- Tiwari, S., & Bahadur, P. (2019). Modified hyaluronic acid based materials for biomedical applications. *International Journal of Biological Macromolecules*, 121, 556–571.
- Todros, S., Todesco, M., & Bagno, A. (2021). Biomaterials and their biomedical applications: from replacement to regeneration. *Processes*, 9.
- Vasi, A. M., Popa, M. I., Butnaru, M., Dodi, G., & Verestiuc, L. (2014). Chemical functionalization of hyaluronic acid for drug delivery applications. *Materials Science* and Engineering C, 38, 177–185.
- Winkler, G. M., Lorenc, Z. P., Öhrlund, Å., & Phd, K. E. (2017). Factors affecting the rheological measurement of hyaluronic acid gel fillers factors affecting the rheological measurement of hyaluronic acid gel fillers. *Journal of Drugs in Dermatology*, 16(9), 876–882.
- Wongprasert, P., Dreiss, C. A., & Murray, G. (2022). Evaluating hyaluronic acid dermal fillers: a critique of current characterization methods. *Dermatologic Therapy*, 35(6), Article e15453.
- Xiang, C., et al. (2022). A porous hydrogel with high mechanical strength and biocompatibility for bone tissue engineering. *Journal of Functional Biomaterials*, 13 (3), 140.
- Xue, B., et al. (2021). Engineering hydrogels with homogeneous mechanical properties for controlling stem cell lineage specification. PNAS, 118(37), Article 211096118.
- Xue, Y., et al. (2020). Synthesis of hyaluronic acid hydrogels by crosslinking the mixture of high-molecular-weight hyaluronic acid and low-molecular-weight hyaluronic acid with 1,4-butanediol diglycidyl ether. RSC Advances, 10, 7206–7213.
- Yang, R., Tan, L., Cen, L., & Zhang, Z. (2016). An injectable scaffold based on crosslinked hyaluronic acid gel for tissue regeneration. RSC Advances, 6, 16838–16850.
- Yasin, A., et al. (2022). Advances in hyaluronic acid for biomedical applications. Frontiers in Bioengineering and Biotechnology, 10, Article 910290.
- Zerbinati, N., et al. (2020). Chemical and mechanical characterization of hyaluronic acid hydrogel cross-linked with polyethylen glycol and its use in dermatology. *Dermatologic Therapy*, 33(4), Article 13747.
- Zerbinati, N., et al. (2021a). Comparative physicochemical analysis among 1,4-butanediol diglycidyl ether cross-linked hyaluronic acid dermal fillers. Gels, 7(3), 1139.
- Zerbinati, N., et al. (2021b). Toward physicochemical and rheological characterization of different injectable hyaluronic acid dermal fillers cross-linked with polyethylene glycol diglycidyl ether. *Polymers (Basel)*, 13(6), 948.
- Zerbinati, N., et al. (2022). Rheological investigation as tool to assess physicochemical stability of a hyaluronic acid dermal filler cross-linked with polyethylene glycol diglycidyl ether and containing calcium hydroxyapatite, glycine and L-proline. *Gels*, 8(5), 264.
- Zhai, P., et al. (2020). The application of hyaluronic acid in bone regeneration. International Journal of Biological Macromolecules, 151, 1224–1239.